Post-synthetic modification mechanism for 1D spin crossover coordination polymers

Alejandro Enriquez-Cabrera, Livia Getzner, L. Salmon, Lucie Routaboul, Azzedine Bousseksou

Post-synthetic modification mechanism for 1D spin crossover coordination polymers

Alejandro Enríquez-Cabrera, Livia Getzner, Lionel Salmon,* Lucie Routaboul,* Azzedine Bousseksou

lionel.Salmon@lcc-toulouse.fr, lucie.routaboul@lcc-toulouse.fr

LCC, CNRS, 205 route de Narbonne, 31077 Toulouse, France

Abstract

In this work we present a comprehensive study of the influence of the solvent on the post-synthetic modification (PSM) on the $[Fe(NH_2trz)_3](NO_3)$ spin crossover (SCO) complex with *p*-anisaldehyde. We demonstrate that the use of a suitable solvent such as ethanol results in a complete PSM, where the final crystalline material exhibits a gradual conversion just below room temperature. In the other hand, when an unsuitable solvent such as toluene or 1-octanol is used, either no reaction or very long reaction time is needed, leading to undesired Fe(III) species. Transmission electronic microscopy analyses show that the complete PSM reaction carried out on nanoparticles of the same complex, changes drastically the size and morphology of the particles.

Introduction

In the last few years the post-synthetic modification (PSM) has emerged as a very important and efficient tool to chemically modify different materials and to synthesize new species that cannot be obtained otherwise.[1] However, the spin crossover (SCO) community has only recently been attracted by this method.[2-13] From the wide variety of SCO complexes available, we have focused on the family of the 1D polymeric iron-triazole complexes, specifically $[Fe(NH_2trz)_3]X_2$ (Figure 1) derived from 4-amino-1,2,4-triazole (aminotriazole), because of their advantages as attractive switchable materials.[14] These compounds present interesting spin crossover properties with hysteretic behavior near room temperature and have been reported as nano-objects and nanocomposites[15] for their potential integration into devices such as thermal displays, sensors, actuators and so on.[16–18]

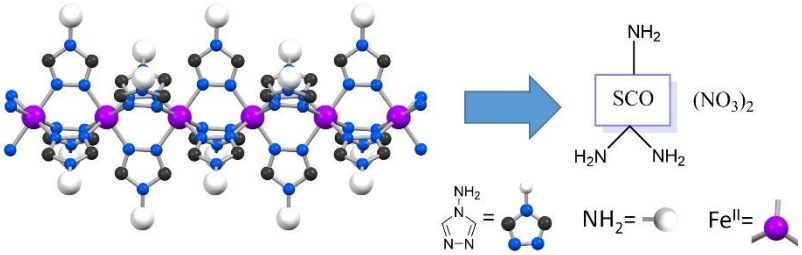

Figure 1.- 1D polymeric structure of the $[Fe(NH_2trz)_3](NO_3)_2$ and its corresponding schematics.

In our previous studies,[4,9] we have demonstrated that a quantitative modification of NH_2 substituents on complexes $[Fe(NH_2trz)_3](X)_2$ (X = NO_3, OTs) can be achieved by PSM reactions with different substrates. Although PSM method was implemented before by Wang et al using the perchlorate derivative (X = ClO_4),[3,7] only low PSM yields (up to 15%) were achieved despite the harsh conditions (24 h reflux in toluene). Besides our studies and the work of Wang, the remaining works on PSM for these aminotriazole complexes were done by either a solid state metathesis reaction[12] (anion exchange) for the chloride derivative (X = Cl) or by exposing the tosylate derivative (X = OTs) in the solid state to a saturated atmosphere of volatile organic compounds such as benzaldehyde.[13] In the last two cases, a complete PSM was observed. These seemingly contradictory results are however a clear illustration of the necessity to consider an ionic compound as a whole, meaning that the counter-ion associated with the central metal is highly important. Indeed, changing the anion not only impacts properties such as solubility, but can also influence the chemical reactivity. For example, exchanging $Cd(NO_3)_2$ with $CdSO_4$

in the same coordination polymer, leads to a change in crystal packing due to a decrease in the coordination number on the metallic center and its Lewis acidic nature. This change of anion yields an increase in the adsorption of large anionic dyes for the sulfate and an increase of catalytical activity for the nitrate.[19] Thus, complexes $[Fe(NH_2trz)_3](X)_2$ are not an exception and their reactivity depends also on the nature of the counteranion. As we have previously demonstrated, a quantitative PSM reaction can be performed for the nitrate and tosylate derivatives (X = NO_3, OTs), while, under the same experimental conditions, no evidence of modification is observed for the sulfate analogue (X = SO_4).[12] It is for this reason that this manuscript focuses on the PSM reaction on the $[Fe(NH_2trz)_3](NO_3)_2$ complex. In particular, the possibility of performing quantitative PSM reactions on an insoluble compound with a compact molecular arrangement is intriguing and prompted us to study its reaction mechanism in detail. Based on examples found in literature concerning the effect of solvents on molecular arrangements as well as on chemical transformations, we expect that the solvent used for the reaction is a key factor in achieving a quantitative PSM reaction.

It is well known that, in molecular systems, the solvent plays an important role on chemical reactivity by affecting: 1) the solubility of the compound; 2) the stability of reactants, intermediate reactive species or the product; 3) the reaction rates which in turn can lead to a better control of product selectivity.[20–22] This has been studied for more complex reactions, e.g. the polymerization of polystyrene[23] and the hydrolysis and reformation of the C-ON bond in alkoxyamines.[24–26]

Intuitively, one might think that a solvent can have no effect on an insoluble solid material but results described in literature show that this assumption is wrong. In more complex or bigger systems (polymers, clusters, MOF's, etc.) the interaction with the solvent is more difficult to study but leads to some very interesting behavior. First, the molecular arrangement of the material can be modified by the presence of solvent. Although not often thought about, a proper interaction of solute and solvent is highly important for various processes such as the nucleation step in the formation of crystals. In materials where the morphology of the solid state is very important (organic solar cells, semiconducting polymers, etc.), the solvent acts as a morphology-directing agent during the processing of the material in the evaporation step[27–31] in addition to being a dissolving agent. Moreover, in the field of spin crossover materials, we have demonstrated that exposing a film to controlled humidity allows for the transformation from pristine to crystalline material in a few seconds.[32,33] This irreversible crystallization process is probably due to hydrogen bonding interactions between water molecules and the complex. Note that the differences in optical properties in the two spin states of the complex are much more pronounced in the crystalline materials than in the pristine ones, which makes them more attractive as switchable materials. Finally, in contrast to the pristine material, the crystalline films are highly reproducible and very stable.[34] Another interesting example on how solvent can interact strongly with a solid material is found in mineral clays. For some of these materials, an exposure to different percentages of relative humidity leads to changes in the structural organization by going from a non-hydrate state up to a tri-hydrate state. The water is allocated in between two sheets of the mineral clays, and with each new inclusion of water the distance between the two sheets increases, leading to some sort of water channels in the mineral clays.[35]

Understanding that the solvent is not inert toward supramolecular assemblies is the first step to use it as a tool to modulate the desired properties or the reactivity of a material. For example: 1) in self-assembled soft materials, solvent enables the formation of chiral superstructures;[36] 2) diblock copolymers can self-assemble in micelles when used in a specific solvent that is active for one of the blocks;[37] 3) core shell polymers can switch in a reversible manner between active and inactive modes depending on the polarity of the solvent used;[38] 4) solvent can also induce a reversible stereochemical

rearrangement in coordination cages, where, for example, the use of nitromethane favors the Δ isomer and acetonitrile favors the Λ isomer.[39]

The molecular arrangement will also have a great influence on the reactivity of solid materials. It is well known that the ternary structure of enzymes or proteins will strongly influence yields and selectivity of biotransformations. Indeed, the nature of the reaction solvent can deeply impact the access to the catalytic site, and the use of unsuitable experimental conditions (temperature, solvent...) results in the deterioration of the enzyme/proteins due to changes in the supramolecular geometry.[40,41] On the other hand, in 1D coordination polymers (1D-CP), the solvent affects the way the CP is arranged, changing its supramolecular architecture[42] or allowing its application as sensors of metal ions[43] by facilitating the exchange of cation, anion and ligands.[44,45] Moreover, this inspired computational scientists to try to simulate the effect of the solvent on supramolecular assemblies. For example, S. Bandyopadhyay et al. computationally investigated the solvent's role in ligand recognition. They conclude that ligand recognition is magnified when the ligand is restricted to move along a specific direction in a small cavity.[46] In addition, solvent molecules are not the only compounds capable of fitting into a molecular arrangement. For example, in 1D-ordered heterostructures if either Na^+ or n-butylammonium cations are located in between silicate layers, delamination in water is not observed, however, this changes drastically when the Na^+ is partially replaced by n-butylammonium, for which rapid delamination occurs when immersed in water.[47] This work also highlights that even if the final and initial states are stable, a small change in the composition of the "sandwich" leads to an increasing rate of delamination of the material.

Thus, for a reaction to take place at the level of a solid compound, it is crucial to allow intermolecular interactions between the active site of the material and the reactants. A well-known method to modify a solid material is mechanochemistry, with which it is possible to perform host-guest chemistry, intercalation of reagents and modification of functional groups in clay-like materials and, in addition, ion exchange on zeolites or smectites.[48] The use of a mechanical force is not the only solution, the presence of certain molecules can also facilitate intermolecular interactions. For example, the choice of solvent can be a crucial point for the success of reactions. PSM methodologies are known to be solvent dependent. Solvent-assisted ligand exchange (SALE)[49–57] is a very interesting example on how a solid that, once formed, is considered inert can be modified in the presence of a solvent. This occurs as a single crystal to single crystal transformation in a heterogeneous manner by incorporating a new linker into the parent material. A quantitative transformation is achieved by placing the starting solid (MOF's,[57,58] COF's,[59] metallic nanoparticles,[54,60,61] perovskites,[30] nanocrystals[62–65] and even quantum dots[66–68]) in a concentrated solution of the linkers.

All of these studies show that even in a compact and insoluble solid, it is possible to perform a complete post-synthetic modification most likely with the aid of the solvent. With this in mind, in this paper, a comprehensive study of the influence of the solvent on the $[Fe(NH_2trz)_3](NO_3)_2$ complex reactivity was performed. Moreover, we present a series of experiments in order to understand the mechanism leading to the complete PSM reaction observed for this compound.

Results and Discussion

In our previous work,[4,9] we have demonstrated that a complete PSM reaction can be performed on the $[Fe(NH_2trz)_3](NO_3)_2$ (**1**) complex with different substrates. However, it was not clear what could be the possible mechanism through which such complete reaction occurs. Based on this, the already well established reaction between **1** and *p*-anisaldehyde, which results in complex [Fe(*p*-MeO-C_6H_4-

CH=Ntrz)$_3$](NO$_3$)$_2$ (**2**), is used as a model to understand and explain the mechanism of this transformation.

1. Verification that the complex **2** is obtained by a PSM method

The fact that the PSM reaction of a compact material is quantitative raises many questions. Some may wonder if the modification of the chemical functions of the complex does not take place in solution instead of between a solubilized reagent and the solid state complex **1** ([Fe(NH$_2$trz)$_3$](NO$_3$)$_2$). A synthetic modification in solution would automatically involve partial or complete decoordination of the aminotriazole ligands from the iron atom (Step A, Scheme 1). In this case the amine function could be converted to an imine function in solution (Step B) and, following this, in the final step the formation of complex **2** can happen through three different pathways: 1) the coordination of the imine ligand to iron nitrate (Pathway C), 2) via ligand exchange of the aminotriazole ligand on complex **1** (Pathway D) or 3) by a transimination reaction with amine in complex **1** (Pathway E).

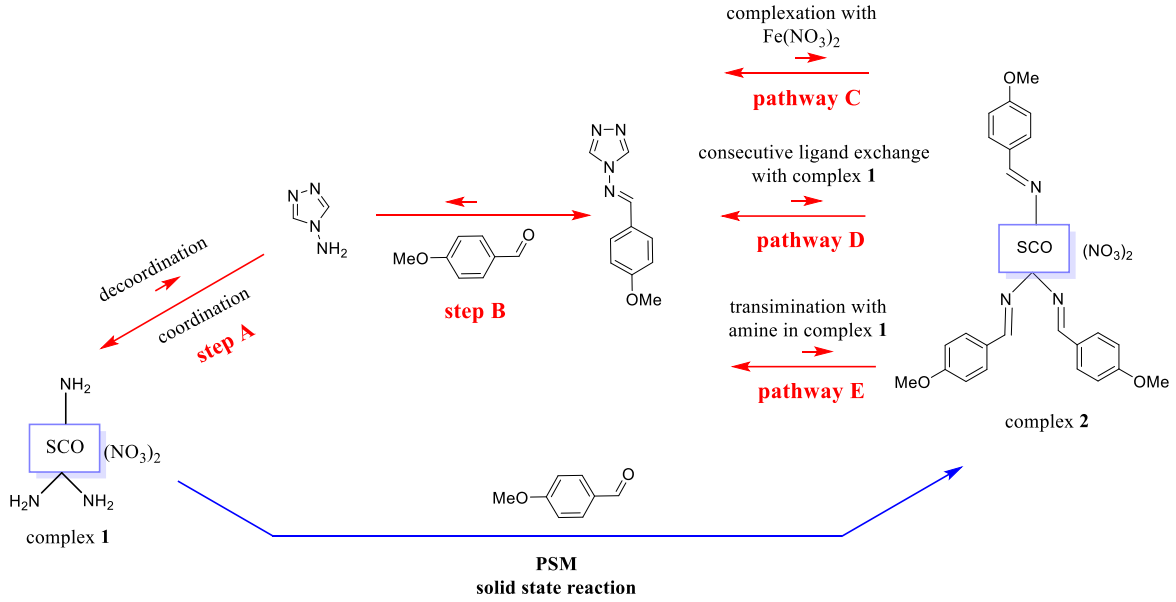

Scheme 1.- Different reaction paths that can lead to the derivative with imine functions (in red reactions that occur in solution, in blue reaction that occur in solid state).

Several experiments were performed to confirm or refute that the modification of the NH$_2$ functions of the compound by reaction with *p*-anisaldehyde is achieved by the PSM methodology. First of all, even though the solubilization of complex **1** was never observed, we heated its suspension in ethanol at 90°C for one hour in order to test the stability of the complex. After filtration at high temperature, the ethanol solution was analyzed by ^{1}H NMR and as expected, no trace of aminotriazole ligand was detected. Similarly, UV studies of the ethanol solution, after filtration of the hot suspension of complex **1,** showed no presence of the ligand or complex **1**. On the other hand, if the suspension of the complex with the imine functions (complex **2**) is heated to 90°C in ethanol, then, by ^{1}H NMR, traces of imine ligands are observed in the ethanol solution (however, the amount of imine is too low to be quantified). These two simple experiments (Scheme S1) indicate that Step A of the reaction pathway in solution can be discarded.

In order to test the feasibility of the last step of the reaction pathway in solution (pathways C, D or E), a reaction between complex **1** (with NH$_2$ functions) and the imine ligand was carried out (Scheme S2).

After one hour at 90°C, complex **1** remained unchanged: no imine functions were detected on the complex by IR spectroscopy, while the ^{1}H NMR of the filtrate solution clearly shows the presence of imine. On the other hand, when complex **2** (with imine functions) is in suspension in ethanol and in the presence of the aminotriazole ligand, after 1 hour at 90°C, a reaction is observed. Indeed, the imine ligand is found in solution and complex **1** is obtained. Thus, a reaction only takes place to transform complex **2** into complex **1**, which is the opposite of what is required for the modification of the amino functions of the compound in solution. Thus, the last step of the reaction pathway in solution is also highly unfavorable.

In a final test, we performed the formation of complex **2** in the presence of a stoichiometric amount of imine ligand (Scheme S3). If the modification of functions is done in solution then the presence of this amount of imine should accelerate the formation of complex **2**. We did not observe any significant change between this reaction and the conventional synthesis of complex **2**, again suggesting that the modification of functions does not occur in solution.

To summarize, all these experiments indicate that the reaction does not take place in solution convincing us that the transformation of the amino functions is indeed the result of a PSM reaction. Therefore, in the following we attempt to explain the mechanism of the quantitative transformation of the rather non-porous complex **1** by demonstrating that, when a suitable solvent is used, the polymeric chains are spaced apart far enough to allow a reaction to take place.

2. Studies on the mechanism of the PSM reaction

Presentation of our working hypothesis

This working hypothesis also has its origins in the structure determined by X-ray diffraction of a single crystal of complex **1**,[69] which is further described in the thesis of Arnaud Grosjean.[70] For the structure of compound **1**, which crystallizes with two water molecules, two types of molecular arrangements can be observed. The first type of arrangement results from direct interactions between polymeric chains through NH_2-NH_2 links. The second type of arrangement shows the interactions of hydrogen bonding between polymer chains and water molecules. In the latter case the water molecules are located in a channel between the polymeric chains, thereby spacing the polymeric chains apart (Figure 2).

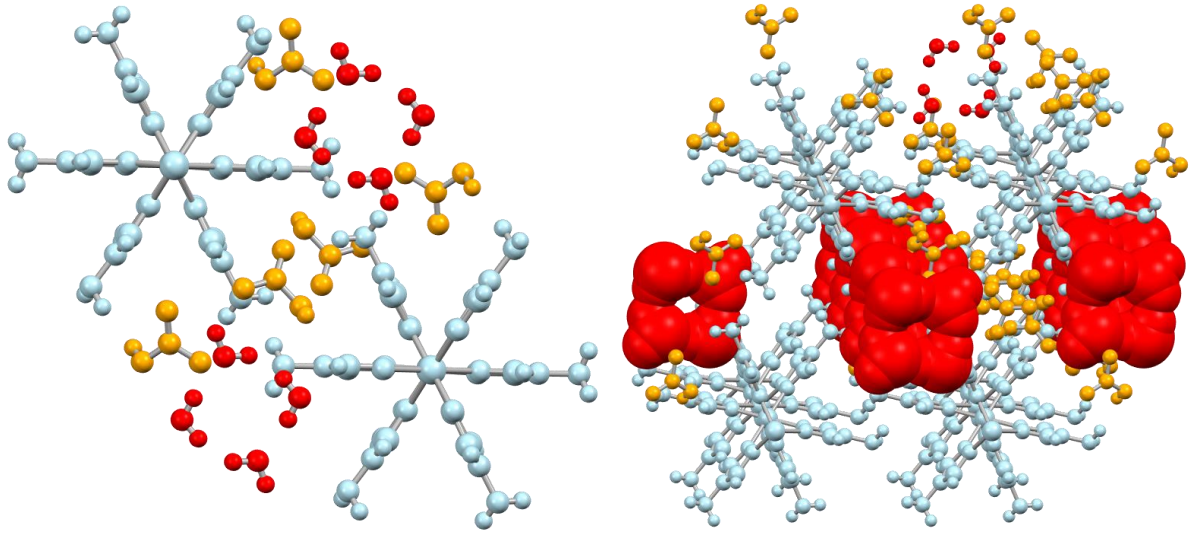

Figure 2.- Crystal structure of complex **1**, where water (in red) is located in channels between the polymeric chains.

Thus, we have good reason to believe that for complex **1** in suspension similar interactions between the polymeric chains of the complex and the solvent are created. In fact, as the powder of complex **1** corresponds to an agglomerate of particles, the first role of the solvent is the separation of the particles of the complex (Figure 3, Step A). This is an important criterion but not yet sufficient to explain the full PSM. If the solvent just separates the powder into single particles, then the PSM reaction can only take place on the surface of said particles (Step B). In this case, a core-shell material would be obtained, with the core composed of iron complex with amine functions and the shell composed of iron complex with imine functions. However, this type of material is not obtained as proven by the different methods of analysis used, which systematically show only one type of population instead of two. Therefore, the second role of the solvent is to separate the polymeric chains that constitute crystallites in the particles (Step C). Taking into account that a polar protic solvent like ethanol might have stronger interactions with the polymeric chains than a nonpolar solvent like toluene, the PSM reaction should be more efficient in ethanol than in toluene, if our working hypothesis is correct.

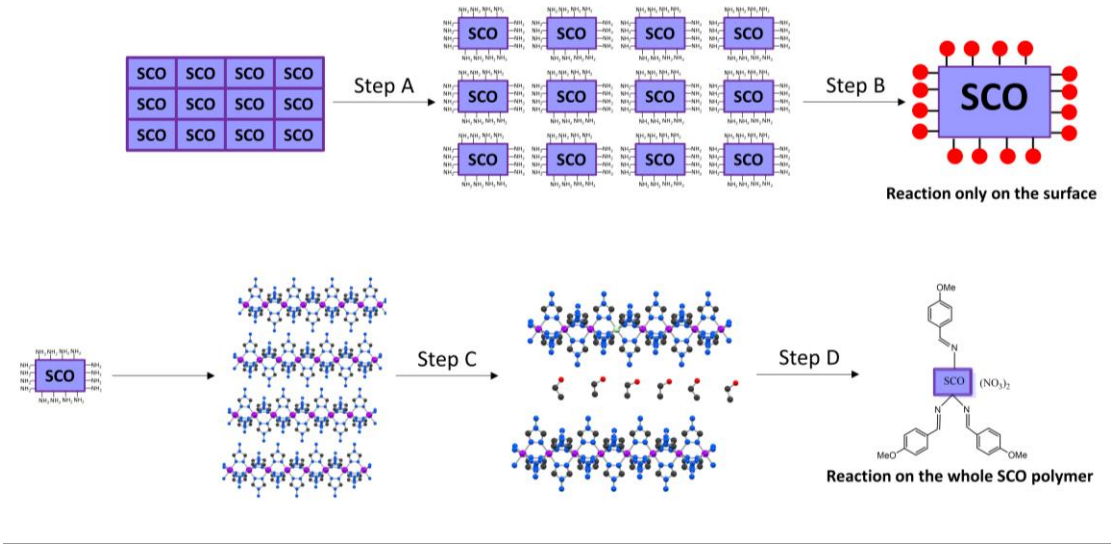

Figure 3.- Sketch representing our working hypothesis.

Influence of solvent in the PSM

In order to confirm or refute our hypothesis, we wanted to test the influence of different solvents on the efficiency of PSM reactions. Therefore, first of all the influence of the nature of the solvent on the formation of the imine ligand (Figure S4) was determined, since it is well known that the rate of an organic transformation can be drastically influenced by the nature of the solvent. This allows us to separate the influence of the solvent on the formation of the imine function from the effect of the solvent on the separation of the polymeric chains and therefore on the PSM efficiency. From this study, we observe that the imine ligand is formed in any solvent tested and that it is formed more rapidly in toluene or octanol than in butanol, ethanol or dioxane.

We then tested the efficiency of PSM in several solvents. Note that, in order to more easily compare the effects of a change of solvent on PSM efficiency, we used the same batch of complex **1** for all experiments. The efficiency of PSM (the percentage of imine/amine) was determined by digestion (see ESI for details) following different reaction times at 90°C. Figure 4a clearly shows that quantitative PSM

is observed within 1 h in absolute ethanol or methanol, while in toluene and dioxane no reaction is observed after 4 h (and even after 12 h). Thus, PSM is clearly more efficient in a polar solvent than in a nonpolar solvent. The drastic difference in efficiency of PSM in polar and nonpolar solvents contrasts with the results obtained for the formation of the imine from the aminotriazole ligand. Thus, this difference is really due to the specific reactivity of the complex and might be explained by the larger space between the polymer chains in the presence of ethanol or methanol. Using alcohols as solvents, we observed that the larger the alkyl chain, the slower the PSM reaction occurs. Two possible explanations are proposed for this result: 1) the lower polarity of the solvent leads to a less efficient PSM reaction; 2) as the length of the alkyl chain increases, the lipophilic character of the solvent increases and therefore its hydrophilicity decreases. Thus, the hydrophilic complex **1** will interact more strongly with ethanol compared to butanol. In addition, it seems that the reaction requires an initiation phase where the first substitutions are more difficult. Only when 20-30% of PSM are obtained, the reaction suddenly becomes much faster. For example, in the case of ethanol, in 30 minutes 35% PSM are obtained, while after 40 minutes more than 80% PSM are reached. This can be rationalized as in addition to the effect of the solvent, the substitution of the first amine functions on the complex **1** increases the space in between the polymeric chains, which, in turn, facilitates the transformation of the other amine functions. Thus, as in reference 47, the transformation of a few NH_2 substituents on complex **1** is sufficient to cause an increasing rate of the modification of the remaining functions. It is worth noting that, when PSM is performed in a 50/50 ethanol/toluene mixture, the complete transformation of the amine functions can be obtained, however, this transformation is much slower than in absolute ethanol and requires 90 minutes of heating before a reaction is observed. Finally, the efficiency of the PSM reaction in absolute ethanol was compared to that performed in 96% ethanol, where the reaction occurs even faster. For example, in 30 minutes, 80% PSM is obtained in 96% ethanol while it is only 35% in absolute ethanol. This shows the large influence of the amount of water in ethanol on the efficiency of the PSM.

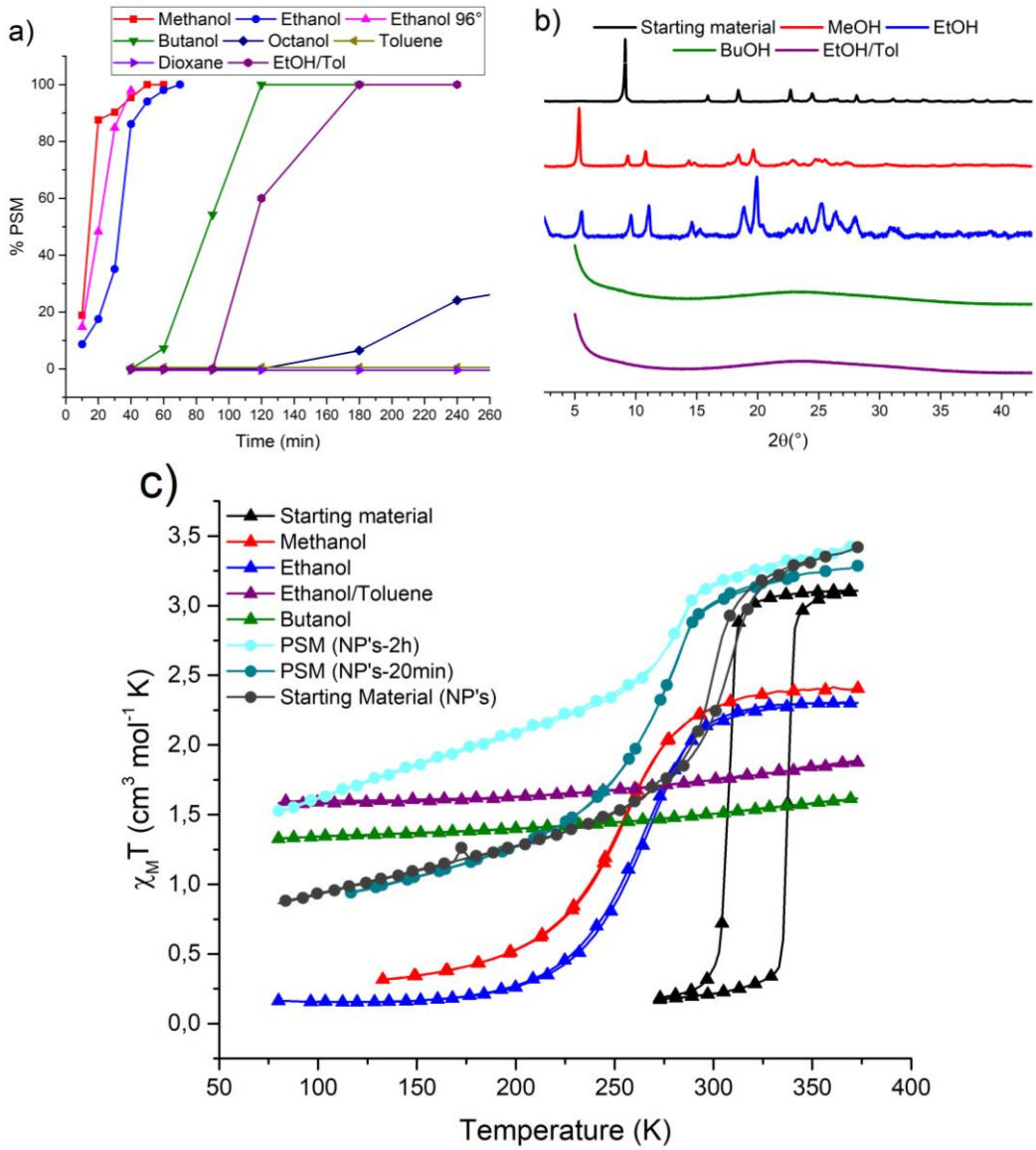

Figure 4- a) Results of the digestion following the PSM reaction performed in different solvents at 90°C; b) PXRD measured at room temperature; c) variable temperature magnetic measurements of the complex after 100% PSM obtained in different solvents for bulk samples and nanoparticles (NP's).

Characterization of the complexes 2 obtained via the PSM method in different solvents

In addition to the study of the influence of the solvent on the efficiency of the PSM, the physicochemical properties of the final compounds obtained in various solvents were analyzed. It should be noted that the color of the materials varies from beige or light yellow (methanol and ethanol) to orange (ethanol/toluene and butanol) and even brown (octanol) depending on the solvent used for the reaction, in agreement with the increasing presence of oxidized iron fractions (see hereafter). The X-ray powder diffraction analysis of the different materials is shown in Figure 4b. For the PSM modification performed in ethanol or methanol, the complex remains crystalline, while complexes obtained in octanol, butanol and the ethanol/toluene mixture are fully amorphous.

Magnetic measurements (Figure 4c) show that the magnetic properties of the obtained compound also depend on the nature of the solvent used for the PSM reaction. In the case of absolute ethanol and methanol a more gradual conversion centered around 257 K and 268 K, respectively, is observed in

comparison with the starting amino derivative, while in the case of the complexes obtained in the ethanol/toluene mixture or in butanol no transition is observed.

Finally, Mössbauer measurements (Figure S3) have been performed on selected materials (at 80 K). In the case of complex **2** obtained in ethanol (1 hour), the iron is mainly in oxidation state II (about 94%) of which about 87% is in the low spin (LS) state, indicating a residual high spin (HS) fraction. On the other hand, in the case of the compound obtained in butanol, the iron is almost completely in oxidation state III (97%). If we take into account the contribution of the different iron states with their corresponding $\chi_M T$ values, the sum of such contributions (0.99 $cm^3mol^{-1}K$) corresponds approximatively to the SQUID measurements at 80 K.

All these analyses indicate that, when the PSM reaction is carried out in ethanol, both the polymeric structure and the degree of oxidation of iron are barely modified. On the other hand, when the reaction is performed in butanol the complex is oxidized and it is not certain that the material is still in the form of long polymers/oligomers. The differences between these two materials can be explained either by the change of solvent or by the longer reaction time needed to obtain a full PSM (100% imine) in butanol. In order to try to determine the reason for these differences, the PSM reaction in ethanol was deliberately carried out for 4 hours. The magnetic measurements and Mössbauer analyses of this new material resemble those of the complex obtained in butanol (Figure S2). Thus, it is reasonable to suggest that the instability comes from the long reaction time. Butanol and octanol are most likely less efficient at separating the polymer chains, thus the longer reaction time, which allows for the oxidation of the gradually formed imine material. Note that complex **1** with amine functions can remain several hours in ethanol at 90°C without degradation.

To conclude this part, the efficiency of the PSM method depends strongly on the nature of the solvent used for the reaction. As expected, in a polar solvent like ethanol, the PSM reaction is quantitative whereas in toluene the reaction does not take place. The long reaction times necessary to obtain the material with 100% imine in butanol and octanol leads to the formation of oxidized species. Thus, these results validate our working hypothesis and demonstrate that in order to obtain the desired material, the choice of a suitable solvent is crucial.

In addition, the PSM reaction on complex **1** changes the steric hindrance of the substituents present on the complex, as the N=CH-C_6H_4-OMe substituent is obviously bulkier than the NH_2 group. This increase in steric hindrance imposed by the substituent could result in a larger distance between the polymeric chains and could explain the evolution of the spin crossover properties from a very cooperative transition with a hysteresis loop in the case of the amino derivative to the gradual conversion observed for the final product.

Moreover, these intermolecular interactions, which control the arrangement of the polymer chains, also have an influence on the interactions between particles of the complex. In particular, it is expected that, the numerous hydrogen bonding type interactions observed in complex **1** will no longer be present in complex **2**. Thus, these modifications could have strong consequences on both the size and the shape of the particles forming the bulk materials.

3. Studies of the influence of the PSM reaction on the size and shape of nanoparticles

For this study we synthesized complex **1** using a reverse micelle method under slightly modified conditions that previously allowed for controlling the size of the nanoparticles in another SCO complex

of the same family (see ESI).[71–73] Subsequently, PSM reactions were carried out on these nanoparticles and quantitative reactions were achieved in 30 minutes using an oil bath or in 20 minutes under microwave activation. Compared to the bulk material (solid compound obtained without particle size control), the PSM reaction is faster for the nanoparticles. This result is not surprising: the smaller the particles, the larger the contact area and thus the faster the reaction. As seen for the bulk material, increasing the time of the PSM reaction led to a darker color of compound **2** (from very light yellow to dark brown for 30 minutes and 2 hours of reaction respectively, both at 90°C in an oil bath).

Figure 5 shows transmission electron microscopy images of nanoparticles of complex **1** as well as the corresponding particles of complex **2** after different PSM reaction times.

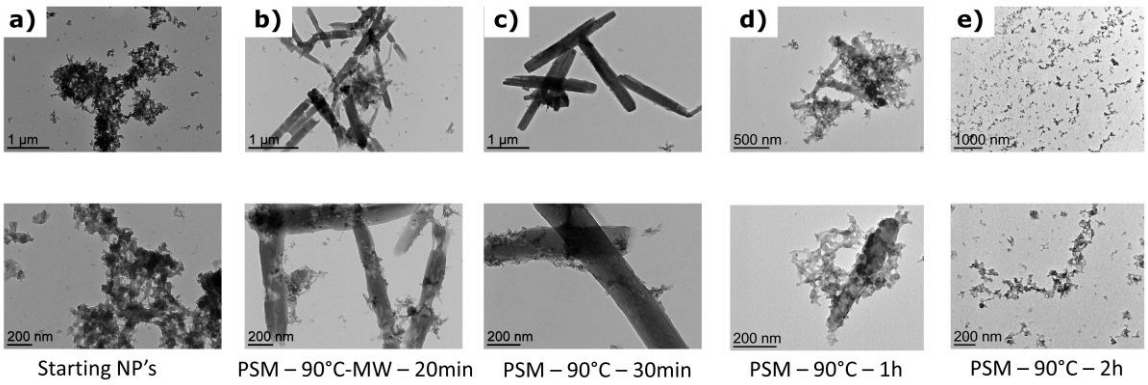

Figure 5: TEM images of nanoparticles of complexes **1** and **2** (top panel, low magnification; bottom panel, high magnification).

TEM images of the starting complex **1** show that the obtained nanoparticles are homogeneous in size (about 50 nm) (Figure 5a). While some isolated nanoparticles can be found, most of the time agglomerates of particles are observed (Figure S3). The size and shape of the particles of complex **2** depend strongly on the time of the PSM reaction. The images for the reaction performed under microwave irradiation for 20 minutes and the reaction done in the oil bath for 30 minutes are similar. They reveal larger size particles than the ones observed for complex **1** and exhibit a rod-like shape. It is important to point out that this change in morphology and particle size is indeed a result of the PSM reaction, because if complex **1** is suspended in ethanol and heated to 90°C, particles of the same size and shape as before heating are observed (Figure S4). The particles of complex **2** (Figure 5b and c) are about 100 nm wide and range in length from 400 nm to 2.2 µm, where the latter most likely corresponds to the direction along the chains iron-iron axis of the complex.[70] This raises the question of how such objects can be obtained from rather spherically shaped nanoparticles of about 50 nm in size. As a reminder, when complex **2** is heated in ethanol, traces of imine ligand are observed in solution and could coordinate to two iron centers of different particles, leading to a morphological reorganization that can explain the large rod-like particles observed when the PSM is complete. However, after 1 h of reaction small spherical particles start to reappear and eventually (after 2 h) only spherical particles of about 20 nm are observed. This could indicate that the particles of complex **2** degrade with increasing reaction times (via decomposition or oxidation), as previously observed for the bulk material.

This TEM study seems to confirm that the PSM reaction does indeed have a significant impact on the particle size and morphology of the complex, as previously hypothesized. Furthermore, the difference in morphology and particle size of complex **2** depending on the reaction time, confirms the degradation of complex **2** over time under these experimental conditions. This observation is in agreement with the one made regarding the PSM reaction time of the bulk compound **1** in ethanol.

Finally, as mentioned before, magnetic measurements were also performed on the nanoparticles (Figure 4c). Firstly, nanoparticles of complex **1** appear to have a less complete SCO transition with a residual HS fraction at low temperatures and a slightly smaller hysteresis loop occurring at a lower temperature than for the corresponding bulk compound. These differences can be explained by the size reduction of the particles.[15] For the particles of complex **2** that were obtained in 20 minutes via a PSM reaction, the amount of switching iron II centers is very similar to the starting nanoparticles of complex **1**, with the same residual HS fraction at low temperature. The SCO behavior is comparable to that observed for the bulk compound **2**, showing a gradual conversion centered around 280 K. For particles of complex **2** obtained by a 2 hour long PSM reaction, a more incomplete spin transition is observed. The partial oxidation of iron II atoms and the size reduction of particles are plausible explanations for the high value of χ_T at low temperature.

Conclusion

In this paper we have demonstrated that the modification of the NH_2 functions present on the complex $[Fe(NH_2trz)_3](NO_3)_2$ was indeed achieved by a post-synthetic modification methodology. We then confirmed that it is possible to perform quantitative PSM reactions on this solid-state complex. The key factor to obtain this result is the use of a suitable solvent (ethanol or methanol). These two solvents limit the interactions between the particles and separate the polymeric chains of the complex, which allows for an efficient contact of the NH_2 functions of the complex with the aldehyde. Note that the use of an unsuitable solvent either leads to no reaction or requires longer reaction times to transform the amine functions into imines. However, in the latter case the resulting compound is not the desired product since the iron II atoms were mostly oxidized to iron III during imine formation. The analysis by transmission electron microscopy confirms that the PSM reaction has a drastic effect on the size and the shape of the nanoparticles and shows that a deterioration of the complex occurs if the reaction time is too long. Thus, this work demonstrates unambiguously that the solvent can have drastic effects on insoluble solid compounds and that the PSM reaction is not restricted to porous solids. Therefore, we show that a careful selection of a suitable solvent is the key step for the success of the PSM methodology for this SCO complex.

Acknowledgment

We thank financial support from the Agence Nationale de la Recherche (ANR-19-CE09-0008-01), AEC thanks the CONACyT (Mexico) for the postdoctoral grant and LG thanks for the Erasmus Scholarship No. 1304753.

References

1 M. Kalaj and S. M. Cohen, *ACS Cent. Sci.*, 2020, **6**, 1046–1057.

2 J. E. Clements, J. R. Price, S. M. Neville and C. J. Kepert, *Angew. Chemie Int. Ed.*, 2014, **53**, 10164–10168.

3 C.-F. Wang, R.-F. Li, X.-Y. Chen, R.-J. Wei, L.-S. Zheng and J. Tao, *Angew. Chemie Int. Ed.*, 2015, **54**, 1574–1577.

4 A. Enríquez-Cabrera, K. Ridier, L. Salmon, L. Routaboul and A. Bousseksou, *Eur. J. Inorg. Chem.*, 2021, **2021**, 2000–2016.

5 C. Ma and C. Besson, *Dalton Trans.*, 2021, **50**, 18077–18088.

6 Y. Komatsumaru, M. Nakaya, F. Kobayashi, R. Ohtani, M. Nakamura, L. F. Lindoy and S. Hayami,

Z. Anorg. Allg. Chem., 2018, **644**, 729–734.

7 C. F. Wang, G. Y. Yang, Z. S. Yao and J. Tao, *Chem. Eur. J.*, 2018, **24**, 3218–3224.

8 S. Kawabata, S. Chorazy, J. J. Zakrzewski, K. Imoto, T. Fujimoto, K. Nakabayashi, J. Stanek, B. Sieklucka and S. I. Ohkoshi, *Inorg. Chem.*, 2019, **58**, 6052–6063.

9 A. Enríquez-Cabrera, L. Routaboul, L. Salmon and A. Bousseksou, *Dalton Trans.*, 2019, **48**, 16853–16856.

10 H. Flötotto, T. Secker, P. Kögerler and C. Besson, *Eur. J. Inorg. Chem.*, 2019, 2–6.

11 L. F. Wang, W. M. Zhuang, G. Z. Huang, Y. C. Chen, J. Z. Qiu, Z. P. Ni and M. L. Tong, *Chem. Sci.*, 2019, **10**, 7496–7502.

12 J. H. Askew and H. J. Shepherd, *Dalton Trans.*, 2020, **49**, 2966–2971.

13 E. Resines-Urien, L. Piñeiro-López, E. Fernandez-Bartolome, A. Gamonal, M. Garcia-Hernandez and J. Sánchez Costa, *Dalton Trans.*, 2020, **49**, 7315–7318.

14 O. Roubeau, *Chem. Eur. J.*, 2012, **18**, 15230–15244.

15 L. Salmon and L. Catala, *Comptes Rendus Chim.*, 2018, **21**, 1230–1269.

16 J.-F. Létard, P. Guionneau and L. Goux-Capes, in *Spin Crossover in Transition Metal Compounds III*, Springer-Verlag, Berlin/Heidelberg, 2006, vol. 1, pp. 221–249.

17 M. Piedrahita-Bello, J. E. Angulo-Cervera, A. Enriquez-Cabrera, G. Molnár, B. Tondu, L. Salmon and A. Bousseksou, *Mater. Horizons*, 2021, **8**, 3055–3062.

18 K. Boukheddaden, M. H. Ritti, G. Bouchez, M. Sy, M. M. Dîrtu, M. Parlier, J. Linares and Y. Garcia, *J. Phys. Chem. C*, 2018, **122**, 7597–7604.

19 N. Kumar and A. K. Paul, *Inorg. Chem.*, 2020, **59**, 1284–1294.

20 J. J. Varghese and S. H. Mushrif, *React. Chem. Eng.*, 2019, **4**, 165–206.

21 C. Reichardt and T. Welton, *Solvents and Solvent Effects in Organic Chemistry*, Wiley-VCH Verlag GmbH & Co. KGaA, Weinheim, Germany, 2010.

22 M. B. Smith and J. March, *March's Advanced Organic Chemistry*, John Wiley & Sons, Inc., Hoboken, NJ, USA, 2006.

23 M. M. Arce, C. W. Pan, M. M. Thursby, J. P. Wu, E. M. Carnicom and E. S. Tillman, *Macromolecules*, 2016, **49**, 7804–7813.

24 G. Audran, P. Brémond, S. R. A. Marque and G. Obame, *Polym. Chem.*, 2012, **3**, 2901.

25 G. Audran, P. Brémond, S. R. A. Marque and G. Obame, *J. Org. Chem.*, 2013, **78**, 7754–7757.

26 E. G. Bagryanskaya, P. Brémond, T. Butscher, S. R. A. Marque, D. Parkhomenko, V. Roubaud, D. Siri and S. Viel, *Macromol. Chem. Phys.*, 2015, **216**, 475–488.

27 Y. Xu, R. Yang, J. Peng, A. A. Mikhailovsky, Y. Cao, T.-Q. Nguyen and G. C. Bazan, *Adv. Mater.*, 2009, **21**, 584–588.

28 C. McDowell, M. Abdelsamie, M. F. Toney and G. C. Bazan, *Adv. Mater.*, 2018, **30**, 1–30.

29 X. Liu, S. Huettner, Z. Rong, M. Sommer and R. H. Friend, *Adv. Mater.*, 2012, **24**, 669–674.

30 J. Woo Choi, H. C. Woo, X. Huang, W.-G. Jung, B.-J. Kim, S.-W. Jeon, S.-Y. Yim, J.-S. Lee and C.-L.

Lee, *Nanoscale*, 2018, **10**, 13356–13367.

31 J. Wang and Z. Liang, *ACS Appl. Mater. Interfaces*, 2016, **8**, 22418–22424.

32 A. C. Bas, V. Shalabaeva, X. Thompson, L. Vendier, L. Salmon, C. Thibault, G. Molnár, L. Routaboul and A. Bousseksou, *Comptes Rendus Chim.*, 2019, **22**, 525–533.

33 V. Shalabaeva, S. Rat, M. D. Manrique-Juarez, A. Bas, L. Vendier, L. Salmon, G. Molnár and A. Bousseksou, *J. Mater. Chem. C*, 2017, **5**, 4419–4425.

34 K. Ridier, A. Bas, Y. Zhang, L. Routaboul, L. Salmon, G. Molnár, C. Bergaud and A. Bousseksou, *Nat. Commun.*, 2020, **11**, 3611.

35 E. Ferrage, B. Dazas, B. Lanson, M. Jiménez-Ruiz, A. Delville and L. J. Michot, *L'Actualité Chim.*, 2016, **413**, 19–25.

36 L. Zhang, L. Qin, X. Wang, H. Cao and M. Liu, *Adv. Mater.*, 2014, **26**, 6959–6964.

37 T.-L. Nghiem, D. Coban, S. Tjaberings and A. H. Gröschel, *Polymers (Basel).*, 2020, **12**, 2190.

38 N. K. Vishwakarma, Y.-H. Hwang, P. R. Adiyala and D.-P. Kim, *ACS Appl. Mater. Interfaces*, 2018, **10**, 43104–43111.

39 W. Xue, T. K. Ronson, Z. Lu and J. R. Nitschke, *J. Am. Chem. Soc.*, 2022, **144**, 6136–6142.

40 A. Ben-Naim, *Biophys. Chem.*, 2003, **105**, 183–193.

41 M. Bekhouche, Université Claude Bernard - Lyon I, 2011.

42 W. L. Leong and J. J. Vittal, *Chem. Rev.*, 2011, **111**, 688–764.

43 B. Dutta, R. Jana, A. K. Bhanja, P. P. Ray, C. Sinha and M. H. Mir, *Inorg. Chem.*, 2019, **58**, 2686–2694.

44 X. Cui, A. N. Khlobystov, X. Chen, D. H. Marsh, A. J. Blake, W. Lewis, N. R. Champness, C. J. Roberts and M. Schröder, *Chem. Eur. J.*, 2009, **15**, 8861–8873.

45 A. Gallego, O. Castillo, C. J. Gómez-García, F. Zamora and S. Delgado, *Eur. J. Inorg. Chem.*, 2014, **2014**, 3879–3887.

46 S. Bandyopadhyay, B. B. Majumdar and J. Mondal, *J. Phys. Chem. B*, 2022, **126**, 2952–2958.

47 M. Daab, S. Rosenfeldt, H. Kalo, M. Stöter, B. Bojer, R. Siegel, S. Förster, J. Senker and J. Breu, *Langmuir*, 2017, **33**, 4816–4822.

48 S. Intasa-Ard, K. Imwiset, S. Bureekaew and M. Ogawa, *Dalton Trans.*, 2018, **47**, 2896–2916.

49 N. Chatterjee and C. L. Oliver, *Cryst. Growth Des.*, 2018, **18**, 7570–7578.

50 O. M. Planes, P. A. Schouwink, J. L. Bila, F. Fadaei-Tirani, R. Scopelliti and K. Severin, *Cryst. Growth Des.*, 2020, **20**, 1394–1399.

51 Y. W. Abraha, C.-W. Tsai, J. W. H. Niemantsverdriet and E. H. G. Langner, *ACS Omega*, 2021, **6**, 21850–21860.

52 L. Huang, M. He, B. Chen and B. Hu, *J. Mater. Chem. A*, 2016, **4**, 5159–5166.

53 M. Gharib, L. Esrafili, A. Morsali and P. Retailleau, *Dalton Trans.*, 2019, **48**, 8803–8814.

54 X. Wang, R. D. Tilley and J. J. Watkins, *Langmuir*, 2014, **30**, 1514–1521.

55 K. Kenyotha, K. Chanapattharapol, S. McCloskey and P. Jantaharn, *Crystals*, 2020, **10**, 599.

56 O. Karagiaridi, W. Bury, J. E. Mondloch, J. T. Hupp and O. K. Farha, *Angew. Chemie Int. Ed.*, 2014, **53**, 4530–4540.

57 D. Yu, Q. Shao, Q. Song, J. Cui, Y. Zhang, B. Wu, L. Ge, Y. Wang, Y. Zhang, Y. Qin, R. Vajtai, P. M. Ajayan, H. Wang, T. Xu and Y. Wu, *Nat. Commun.*, 2020, **11**, 927.

58 R. A. Peralta, M. T. Huxley, J. Albalad, C. J. Sumby and C. J. Doonan, *Inorg. Chem.*, 2021, **60**, 11775–11783.

59 Y. Shi, X. Zhang, H. Liu, J. Han, Z. Yang, L. Gu and Z. Tang, *Small*, 2020, **16**, 1–7.

60 R. G. Ellis, J. W. Turnley, D. J. Rokke, J. P. Fields, E. H. Alruqobah, S. D. Deshmukh, K. Kisslinger and R. Agrawal, *Chem. Mater.*, 2020, **32**, 5091–5103.

61 C.-T. Kuo, C.-F. Chen, M.-W. Gu, M.-N. Su, J.-F. Huang, M.-J. Huang and C. Chen, *Chem. Asian J.*, 2014, **9**, 844–851.

62 S. Jeon, J. Ahn, H. Kim, H. K. Woo, J. Bang, W. S. Lee, D. Kim, M. A. Hossain and S. J. Oh, *J. Phys. Chem. C*, 2019, **123**, 11001–11010.

63 M. A. Boles, D. Ling, T. Hyeon and D. V. Talapin, *Nat. Mater.*, 2016, **15**, 141–153.

64 S. L. Abiodun, M. Y. Gee and A. B. Greytak, *J. Phys. Chem. C*, 2021, **125**, 17897–17905.

65 S. Jharimune, A. A. Sathe and R. M. Rioux, *J. Phys. Chem. C*, 2021, **125**, 12792–12801.

66 S. Cho, J. Kim, S. M. Jeong, M. J. Ko, J.-S. Lee and Y. Kim, *Chem. Mater.*, 2020, **32**, 8808–8818.

67 P.-R. Chen, K.-Y. Lai, C.-W. Yeh and H.-S. Chen, *ACS Appl. Nano Mater.*, 2021, **4**, 3977–3988.

68 J. H. Song, H. Choi, Y.-H. Kim and S. Jeong, *Adv. Energy Mater.*, 2017, **7**, 1700301.

69 A. Grosjean, N. Daro, B. Kauffmann, A. Kaiba, J. F. Létard and P. Guionneau, *Chem. Commun.*, 2011, **47**, 12382–12384.

70 A. Grosjean, Université de Bordeaux 1, 2013.

71 I. Suleimanov, J. S. Costa, G. Molnár, L. Salmon, I. Fritsky and A. Bousseksou, *French-Ukrainian J. Chem.*, 2015, **3**, 66–72.

72 Y. Zan, L. Salmon and A. Bousseksou, *Nanomaterials*, 2021, **11**, 3169.

73 R. Torres-Cavanillas, L. Lima-Moya, F. D. Tichelaar, H. W. Zandbergen, M. Giménez-Marqués and E. Coronado, *Dalton Trans.*, 2019, **48**, 15465–15469.